Published June 24, 2014

Journal of Environmental Quality TECHNICAL REPORTS
BIOREMEDIATION AND BIODEGRADATION

Treatment of Dissolved Perchlorate, Nitrate, and Sulfate Using Zero-Valent Iron and Organic Carbon

YingYing Liu, Carol J. Ptacek,* David W. Blowes

Waters containing ClO_4^- and dissolved NO_3^-, derived from detonated explosives and solid propellants, often also contain elevated concentrations of other dissolved constituents, including SO_4^{2-}. Four column experiments, containing mixtures of silica sand, zero-valent Fe (ZVI) and organic C (OC) were conducted to evaluate the potential for simultaneous removal of NO_3^-, SO_4^{2-} and ClO_4^-. Initially, the flow rate was maintained at 0.5 pore volumes (PV) d^{-1} and then decreased to 0.1 PV d^{-1} after 100 PV of flow. Nitrate concentrations decreased from 10.8 mg L^{-1} (NO_3–N) to trace levels through NO_3^- reduction to NH_4^+ using ZVI alone and through denitrification using OC. Observations from the mixture of ZVI and OC suggest a combination of NO_3^- reduction and denitrification. Up to 71% of input SO_4^{2-} (24.5 $\pm$ 3.5 mg L^{-1}) was removed in the column containing OC, and >99.7% of the input ClO_4^- (857 $\pm$ 63 μg L^{-1}) was removed by the OC- and (ZVI + OC)-containing columns as the flow rate was maintained at 0.1 PV d^{-1}. Nitrate and ClO_4^- removal followed first-order and zero-order rates, respectively. Nitrate >2 mg L^{-1} (NO_3–N) inhibited ClO_4^- removal in the OC-containing column but not in the (ZVI + OC)-containing column. Sulfate did not inhibit ClO_4^- degradation within any of the columns.

J. Environ. Qual. 43:842–850 (2014)
doi:10.2134/jeq2013.03.0077
Received 5 Mar. 2013.
*Corresponding author (ptacek@uwaterloo.ca).

PERCHLORATE is a common contaminant in groundwater and surface water. Approximately 90% of ClO_4^- salts are manufactured as NH_4ClO_4, which is widely used in large volumes of solid propellants for rockets, missiles, explosives, and pyrotechnics. A variety of non-military sources, such as the use and manufacture of road flares, $HClO_4$ and $HClO_3$, fireworks displays, and blasting agents used in mining and construction, can also cause widespread, low-concentration ClO_4^- contamination in water. In addition to these anthropogenic sources, naturally occurring ClO_4^- generated via atmospheric processes and contained in NO_3 fertilizers and some natural minerals also contributes low levels of ClO_4^- in some parts of the world (Ward, 2008).

Perchlorate is highly soluble, mobile, and recalcitrant in the environment. It is potentially toxic to various forms of life, with low concentrations inhibiting I^- uptake in human and animal thyroid glands (Leung et al., 2010). Due to these health impacts, the USEPA adopted the National Research Council recommended reference dose of 0.0007 mg kg^{-1} d^{-1} for ClO_4^- as an interim health limit in 2005, which translates to a drinking water equivalent level of 24.5 μg L^{-1}.

Physical-chemical treatment technologies, such as ion exchange, C adsorption, and advanced oxidation are effective for treating a range of contaminants but are less cost efficient and effective for removing ClO_4^- from water (Srinivasan and Sorial, 2009). Ion exchange, a widely accepted water treatment technology, can effectively remove ClO_4^- from water; however, the highly saline (7–12%) brine generated during the ion-exchange process requires costly management before disposal (Okeke et al., 2002). Microbial reduction of ClO_4^- is an area of intense interest because this strategy is relatively cost effective and environmentally compatible (Gal et al., 2008; Okeke and Frankenberger, 2005). The hazardous ClO_4^- is converted into two innocuous compounds—Cl^- and O_2—catalyzed by at least two separate enzymes (Xu et al., 2003).

Perchlorate and NO_3^- are often found as co-contaminants in water because a large number of propellants, blasting agents, and explosives contain ClO_4^- as well as N-containing compounds. Moreover, NO_3–containing compounds, such as KNO_3 and $NaNO_3$, are widely used in agriculture and ClO_4^-–containing

Dep. of Earth and Environmental Sciences, 200 University Avenue West, Univ. of Waterloo, Waterloo, ON, Canada N2L 3G1. Assigned to Associate Editor Scott Young.

Abbreviations: ZVI, zero-valent iron; OC, organic carbon; PV, pore volumes.

pyrotechnics. High concentrations of SO_4^{2-}, derived from S^{2-} oxidation at some mining sites, also require management. Because ClO_4^-– and NO_3–containing blasting agents and explosives are used at mine sites, water containing co-mingled ClO_4^-, NO_3^-, and SO_4^{2-} can develop (Bailey et al., 2013; Ward, 2008). Bioremediation of ClO_4^-– and NO_3^-– contaminated water has been widely studied using various electron donors, such as H_2 or ethyl acetate gases (Evans and Trute, 2006), edible oil (Borden, 2007, Hunter, 2002), compost and mulch mixtures (Wang et al., 2013), and wood particle media (Robertson et al., 2007). The purpose of this study was to identify an effective, economical, and feasible technology to remediate ClO_4^-–, NO_3^-–, and SO_4^{2-}–contaminated waters associated with mining and blasting sites. A series of column experiments was conducted using mixtures of zero-valent Fe (ZVI) and wood chips (OC) as reactive media to remove co-mingled ClO_4^-, NO_3^-, and SO_4^{2-} in simulated groundwater.

Material and Methods

Column Design and Experimental Setup

Four acrylic columns were used, each 30 cm in length with an internal diameter of 5 cm. Influent ports were located at the base of each column, and effluent ports were located at the top of each column for discharge of the effluent solution and for sample collection. In addition, 13 equally spaced sampling ports were installed at approximately 2.1-cm intervals along the length of the columns. Both the bottom and top layers of the four columns were packed with a 1.0-cm-thick layer of silica sand as a nonreactive material to separate the reactive mixture from the influent and effluent end ports.

Column 1 was packed with 100% silica sand (SS) as a control. Column packings were composed of 50% (v/v) granular ZVI with the balance as SS (Column 2), 50% (v/v) wood chips (OC) with the balance as SS (Column 3), and a mixture of 10% (v/v) ZVI and 40% (v/v) OC adjusted with 50% (v/v) SS (Column 4). The granular ZVI (0.17–1.41 mm) was obtained from Connelly-GPM. The silica sand (0.6–0.8 mm) was obtained from the Silica Company. The wood chips (~1–9.5 mm, deciduous hardwood) were obtained from a lumber producer in Waterloo, ON. Before initiating the experiments, all four columns were placed in an anaerobic glove box (COY Ltd.) that contained 5% H_2 and 95% N_2. The columns were flushed with $CO_{2(g)}$, which is more soluble in water than N_2 or O_2, for 24 h to displace atmospheric gases from the void pore space of the column packing and enhance saturation of the packing material. The columns were then wet with simulated groundwater, composed of $CaCO_3$–saturated water during a 48-h period.

A conservative tracer test was performed to determine the flow and transport characteristics of each column. The computer code CXTFIT 2.0 (Toride et al., 1995), a series of analytical solutions to the one-dimensional advection–dispersion equation with nonlinear, least-squares parameter optimization, was used to determine the average linear velocities and dispersion coefficients from the column effluent concentration data. The flow rates of the column experiments were approximately 0.5 pore volumes (PV) d^{-1} during the conservative tracer test.

The input solution was prepared by adding NO_3^-, SO_4^{2-}, and ClO_4^- to the $CaCO_3$–saturated water as Na salts to obtain concentrations of 10.8 ± 0.3 mg L^{-1} NO_3–N, 24.5 ± 3.5 mg L^{-1} SO_4^{2-}, and 857 ± 63 μg L^{-1} ClO_4^-. The ratios of concentrations were based on measurements of effluent from test-scale waste-rock piles (Bailey et al., 2013). The purpose of using $CaCO_3$–saturated water as the input solution was to simulate the presence of HCO_3^- and CO_3^{2-}, which are common in natural surface water and groundwater. Before introducing the input solution, Columns 3 (OC) and 4 (ZVI + OC) were saturated with a solution containing 5% (v/v) sodium lactate for 3 d to promote the growth of microorganisms (Lindsay et al., 2011). The input solution initially was displaced through the four columns from the bottom to the top at a flow rate of 0.5 PV d^{-1} during the first stage of the experiment. During the second stage of the experiment, the flow rates were decreased to 0.1 PV d^{-1} (after 99 PV in Column 2, 112 PV in Column 3, and 110 PV in Column 4) to evaluate the effect of residence time on contaminant removal. Three profiles were collected along the columns during the course of the experiments: after 95.4, 115, and 129 PV of flow passed through Column 2 (ZVI); after 108, 132, and 151 PV of flow through Column 3 (OC); and after 106, 128, and 144 PV of flow through Column 4 (ZVI + OC). During the experiment, there were no obvious signs of clogging or changes in hydraulic conductivity.

Sample Collection and Analytical Methods

Water samples were collected using 30-mL glass syringes attached directly to the ports along the length of the columns and to the effluent ports so that the syringes were filled at the same rate as the input solution being introduced to the columns. Except where noted, all samples were passed through 0.45-μm cellulose acetate filters before measurement. The pH, Eh, and alkalinity were determined immediately after sampling. All other samples were kept chilled (<4°C) until analysis within 1 mo of collection.

Values of pH and Eh were measured on unfiltered samples in sealed cells to minimize O_2 exposure. The pH measurements were made using a Ross combination glass electrode (Orion 815600) calibrated using standard pH 4.0 and 7.0 buffers and then checked against a pH 10.0 buffer. The Eh measurements were made using a Pt-billeted Ag–AgCl combination electrode (Orion 9678BNWP). The performance of the electrode was checked using Zobell's (Nordstrom, 1977) and Light's (Light, 1972) solutions before and after each measurement. Measurements were corrected to the standard H_2 electrode. Alkalinity was determined using a Hach digital titrator with bromocresol green/methyl red indicator and 0.08 mol L^{-1} H_2SO_4.

The concentrations of major anions (Br^-, NO_3^-, NO_2^-, Cl^-, and SO_4^{2-}) were determined by ion chromatography (DX600, Dionex). Ammonia (NH_3–N) concentrations were determined using a Hach spectrophotometer DR/8400 following the salicylate method (APHA, 2005). Dissolved H_2S was determined using the methylene blue spectrophotometric method (Lindsay and Baedecker, 1988).

Filtered 20-mL samples were collected separately in 30-mL polyethylene bottles for ClO_4^- analysis. A headspace was maintained in these sample bottles to minimize the possibility of anaerobic conditions developing during storage. Perchlorate was analyzed following the method described by Snyder et

al. (2005) with the addition of equal aliquots of isotopically enriched sodium perchlorate ($NaCl^{18}O_4$, Cambridge Isotope Laboratories) to all the samples and calibration standards as an internal standard. All water samples were prepared by elution through one OnGuard-II Ba cartridge and one OnGuard-II H cartridge (Dionex) in series to remove SO_4^{2-} and CO_3^{2-}, respectively. Perchlorate was analyzed by high performance liquid chromatography (Agilent 1100, Agilent Technologies) followed by electrospray tandem mass spectrometry (4000 Q TRAP, Applied Biosystems) and detected by negative electrospray ionization mass spectrometry using multiple reaction monitoring detection. The instrument and practical detection limits were 0.02 and 0.05 μg L^{-1}, respectively. Quality assurance/quality control results showed that relative method recovery across the entire standard curve (0.5–100 μg L^{-1}) fell into the range of 98 to 110%, and the relative internal standard recovery for unknown samples was 71 to 118%.

Results and Discussion

Conservative Tracer Test and Control Column Results

The transport model CXTFIT 2.0 was used to determine the velocity and dispersion coefficient for each column during the first stage of the experiments. The fitted velocities estimated by CXTFIT using the Br^- breakthrough curve data ranged from 40.3 to 54.3 m yr^{-1} for the four columns. These values were in agreement with the average linear velocities calculated from porosity and flow volume measurements, which ranged from 49.1 to 59.6 m yr^{-1}, with the exception of Column 2 (ZVI). The dispersion coefficients ranged from 0.1 to 1.2 m^2 yr^{-1} for the four columns (Table 1). Measurements made on the control column indicated that transport of ClO_4^-, NO_3^-, and SO_4^{2-} was conservative (Fig. 1)

Geochemical Conditions of Columns

The three pH profiles within Columns 2 to 4 measured at different times almost overlapped, exhibiting similar values with distance (Fig. 2). The influent water pH value was 8.3 throughout the experiments. The average pH value within Column 2 (ZVI) was 9.7. The increase in pH was due to the reduction of water by the ZVI. The average pH in Column 4 (ZVI + OC) was slightly lower at 8.6. The pH of Column 3 (OC), which did not contain ZVI, was much lower at pH 7.4. Similarly, the average pH of the column effluent was 9.7 in Column 2 and 7.2 in Column 3, remaining within 0.5 pH unit throughout the entire experiment (Fig. 3). The effluent pH of Column 4 increased quickly from below 7 to about 9.5 during the first 10 PVs and then decreased to about 8.6 for the remainder of the first stage of the experiment.

The three alkalinity profiles for each of Columns 2, 3, and 4 indicated similar average values and changing trends, with slight increases as the input solution advanced through the columns (Fig. 2). Total alkalinities with an average value of 96 mg L^{-1} (as $CaCO_3$) were generated in Column 2 (ZVI) effluent; in the effluent of the columns containing OC, slightly higher alkalinity values of 119 mg L^{-1} (as $CaCO_3$) in Column 3 (OC) and 113 mg L^{-1} (as $CaCO_3$) in Column 4 (ZVI + OC) were observed (Fig. 3).

The Eh values in Columns 2, 3, and 4 ranged from moderately oxidizing to moderately reducing conditions during the course of the experiments, with lower values observed during the second stage of the experiments when the flow rates were lower (Fig. 2). Higher average Eh values of ~300 mV were observed within Column 3 (OC) relative to the values observed in the middle distances in Columns 2 (ZVI, −200 mV) and 4 (ZIV + OC, −400 mV). Addition of the lactate solution to Columns 3 and 4 probably resulted in the relatively low Eh and high alkalinity values in the column effluent at the beginning of the first stage of the experiment compared with Column 2 (Fig. 3). In the effluent of Columns 2 and 4 (Fig. 3), the Eh values were relatively constant throughout the experiment. The Eh values in the effluent of Column 3 gradually increased from approximately 40 mV at 35 PV to 460 mV at 110 PV in the first stage of the experiment and then decreased to the average value of 200 mV in the second stage of the experiment. These decreases in Eh values were probably due to the decrease in flow rate from 0.5 PV d^{-1} in the first stage of the experiment to 0.1 PV d^{-1} in the second stage of the experiment.

Removal of Nitrate, Sulfate, and Perchlorate in Columns

Reduction of NO_3^- by ZVI has been observed to proceed rapidly through NO_2^- to NH_4^+. The proposed pathway for the overall reaction is (Rahman and Agrawal, 1997)

$$NO_3^- + 4Fe^0 + 10H^+ \rightarrow 4Fe^{2+} + NH_4^+ + 3H_2O \quad [1]$$

Nitrate was almost completely removed in the column containing ZVI (Column 2), from the average input concentration of 10.8 mg L^{-1} (NO_3–N) to a trace concentration. Nitrite concentrations remained <0.02 mg L^{-1} (NO_2–N) and the average NH_4^+ concentration was 10.7 mg L^{-1} (NH_3–N), indicating that NH_4^+ was the principal byproduct throughout the experiment (Fig. 1). The concentrations of total N (sum of

Table 1. Physical characteristics of the columns used in this study, including a control and columns containing zero-valent Fe (ZVI), organic C (OC), or both.

	Column 1 Control	Column 2 ZVI	Column 3 OC	Column 4 ZVI + OC
Bulk density, g cm^{-3}	1.73	2.27	1.34	1.59
Porosity	0.35	0.40	0.45	0.41
Pore volume, cm^3	219	248	273	246
Average linear velocity, m yr^{-1}	59.6	51.7	50.8	49.1
Fitted velocity, m yr^{-1}	54.3	40.3	49.1	46.4
Dispersion coefficient, m^2 yr^{-1}	0.07	1.16	0.94	0.46
R^2	0.999	0.989	0.995	0.997
Residence time, d	2.02	2.72	2.23	2.36

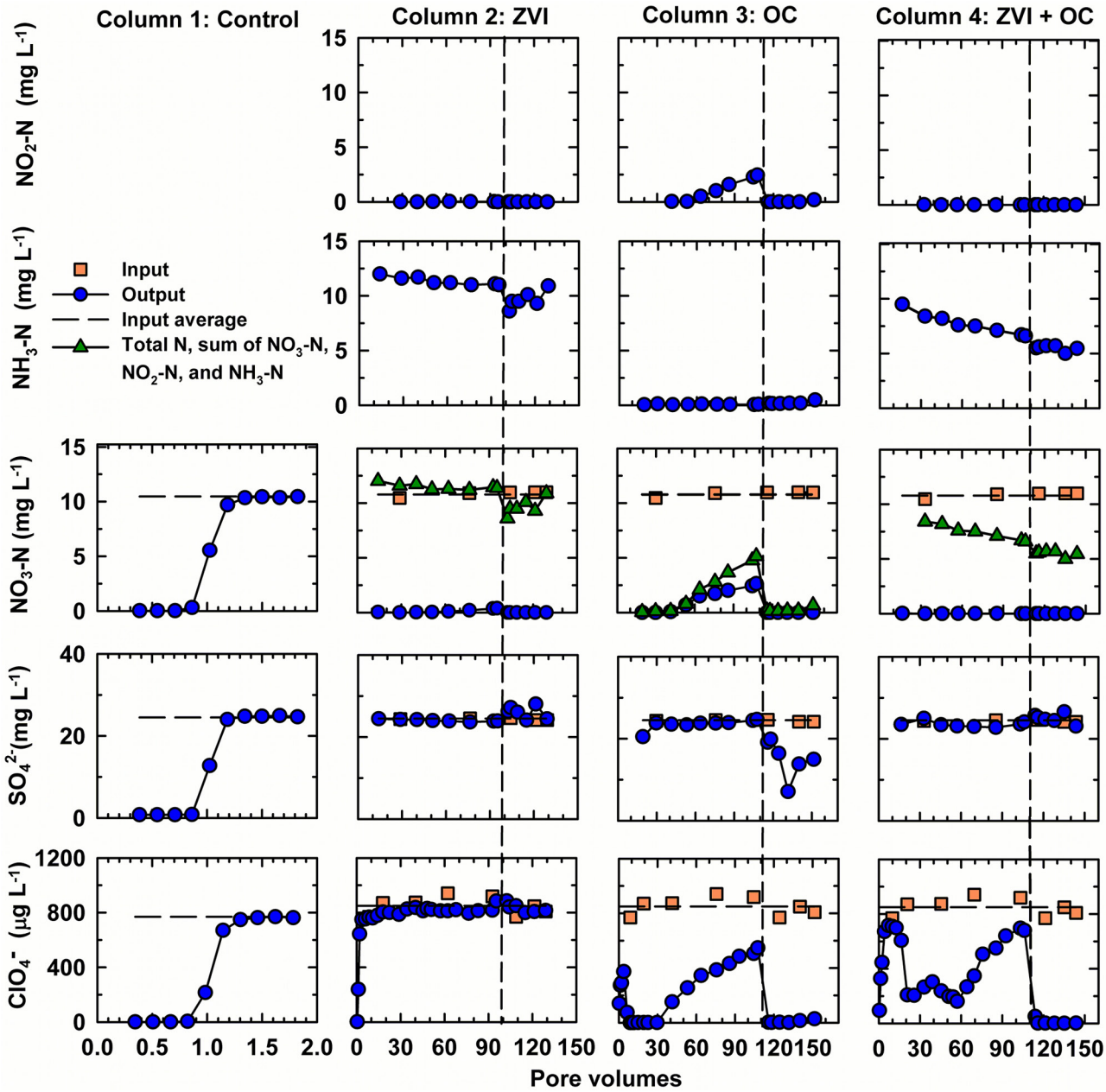

Fig. 1. Concentrations of NO_2–N, NH_4–N, NO_3–N, SO_4^{2-}, and ClO_4^- as a function of pore volumes in effluent from columns containing zero-valent Fe (ZVI), organic C (OC), or both; the dashed lines indicate a change in flow rate in each column, dividing the experiment into two stages.

NO_3–N, NO_2–N, and NH_3–N) in Column 2 (ZVI) effluent were consistent with the input NO_3^- concentrations, indicating complete conversion of NO_3^- to NH_4^+.

Bacterially mediated denitrification by OC such as wood waste as a C source is thermodynamically favored and leads to the stepwise reduction of NO_3^- to form N_2 gas:

$$NO_{3(aq)}^- \rightarrow NO_{2(aq)}^- \rightarrow NO_{(enzyme\ complex)} \rightarrow N_2O_{(gas)} \rightarrow N_{2(gas)} \quad [2]$$

The overall reaction can be expressed as (Appelo and Postma, 2005)

$$5CH_2O + 4NO_3^- \rightarrow 2N_2 + 5HCO_3^- + H^+ + 2H_2O \quad [3]$$

The removal of NO_3^- in Column 3 containing OC was variable (Fig. 1). In the first stage of the experiment (108 PV) at a flow rate of 0.5 PV d^{-1}, up to 2.6 mg L^{-1} NO_3–N remained in the effluent. In addition, up to 2.4 mg L^{-1} NO_2–N, an intermediate reaction product, was observed in the effluent in the first stage of the experiment. However, NO_3^- was more completely removed in the second stage of the experiment when the flow rate decreased to 0.1 PV d^{-1}, from an average input concentration of 10.8 to <0.02 mg L^{-1} (NO_3–N) without measurable NO_2^- observed. A trace of NH_3 (average value 0.1 mg L^{-1} NH_3–N) was observed in the Column 3 effluent samples, perhaps due to the decomposition of OC. In the first stage of the experiment, the total N concentrations in the Column 3 (OC) effluent progressively rose from 0.1 to 5.2 mg L^{-1}. The increase in total N concentrations was predominantly due to an increase in the concentrations of NO_3^- and NO_2^-, indicating that the increase in total N was due to incomplete denitrification, possibly due to a

depletion of labile OC. In the second stage of the experiment, the total N concentration decreased to as low as 0.7 mg L^{-1} N, suggesting that the rate of OC consumption was sufficient to result in complete denitrification during this stage.

The mixture of ZVI + OC in Column 4 resulted in extensive removal of NO_3^-, no detectable release of NO_2^- and the release of 9.5 mg L^{-1} of NH_3–N at the beginning of the experiment that gradually decreased to 6.6 mg L^{-1} at 100 PV (Fig. 1). This decreasing trend suggests that NO_3^- reduction by ZVI predominated early in the experiment and that denitrification became established, resulting in partial conversion of NO_3^- to $N_{2(g)}$. In Stage 2, the average total N concentration was 5.5 mg L^{-1}, almost exclusively as NH_4^+, indicating an increase in the extent of denitrification as the residence time increased, resulting in approximately equal removal by NO_3^- reduction and denitrification. Less NH_4^+ has been observed when ZVI was used in conjunction with a microbial consortia to reduce NO_3^- (Till et al., 1998).

Effluent SO_4^{2-} concentrations did not decrease in the columns containing ZVI (Column 2) or the mixture of ZVI + OC (Column 4) during the experiment (Fig. 1). Sulfate was observed to break through Column 3 (OC) in the first stage of the experiment; however, effluent SO_4^{2-} concentrations in Column 3 decreased from 24.7 mg L^{-1} after 108 PV in the first stage of the experiment to 7.1 mg L^{-1} after 132 PV in the second stage of the experiment (when the flow rate slowed), with approximately 71% of the input SO_4^{2-} (24.5 mg L^{-1}) removed. The effluent SO_4^{2-} concentration then increased to 15.0 mg L^{-1} after 151 PV in the second stage of the experiment. This SO_4^{2-} removal is attributed to the onset of biologically mediated SO_4^{2-} reduction coupled to OC oxidation (Blowes et al., 2000):

$$2CH_2O + SO_4^{2-} \rightarrow 2HCO_3^- + H_2S \quad [4]$$

The decrease in the rate of SO_4^{2-} removal with time was probably due to depletion of labile OC during the long-term operation of the experiment. The inhibition of SO_4^{2-} reduction observed in Column 4 (ZVI + OC) might be attributed to the higher pH conditions developed in this column compared with Column 3 (OC) (Fig. 2 and 3).

Although reduction of ClO_4^- by ZVI is thermodynamically favored, with the Gibbs free energy $\Delta G^0 = -596.27$ kcal mol^{-1}, ClO_4^- was not removed by ZVI in Column 2 throughout the experiment; this was probably due to the high activation energy required for ClO_4^- reduction (Yu et al., 2006). The effluent ClO_4^- concentration was 857 ± 63 μg L^{-1}, similar to the input concentration (Fig. 1). The total effluent Cl concentrations (sum of ClO_4^- and Cl, in μmol L^{-1}) in Column 2 (ZVI) were much higher than the input ClO_4^- concentrations, this difference may be due to the release of Cl initially present on the ZVI (Fig. 4). The presence of Cl in the first pore volumes of flow probably represented residual from the ZVI manufacturing processes.

The effluent concentrations of ClO_4^- in Column 3 decreased from 547 μg L^{-1} after 108 PV in the first stage of the experiment to 28 μg L^{-1} after 151 PV in the second stage of the experiment

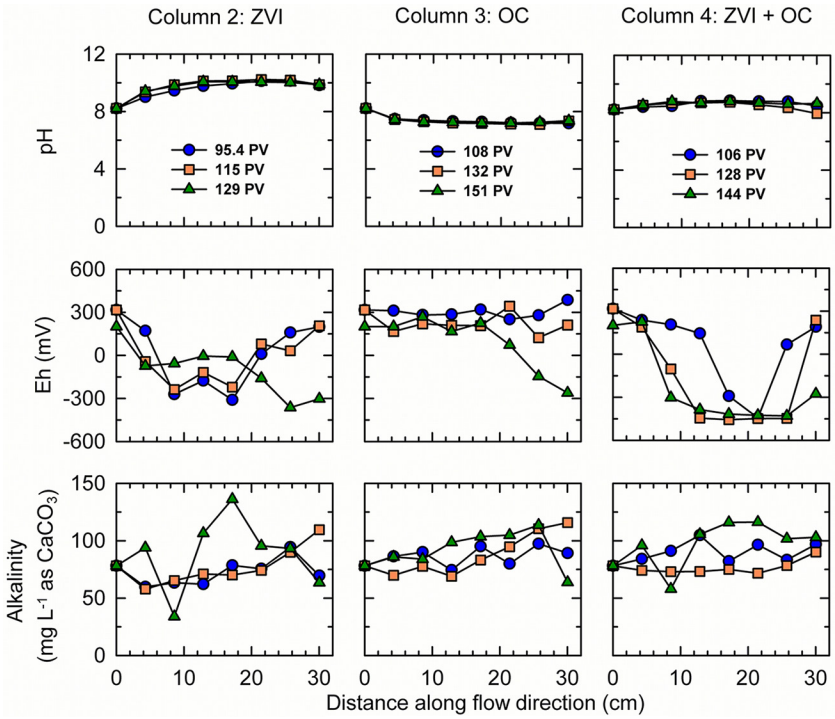

Fig. 2. Values of pH, Eh, and concentrations of alkalinity as a function of distance along the flow direction within the columns containing zero-valent Fe (ZVI), organic C (OC), or both. Blue circle symbols represent data collected during the first stage of the experiment, while orange square and green triangle symbols represent data collected during the second stage of the experiment, given in terms of pore volumes (PV).

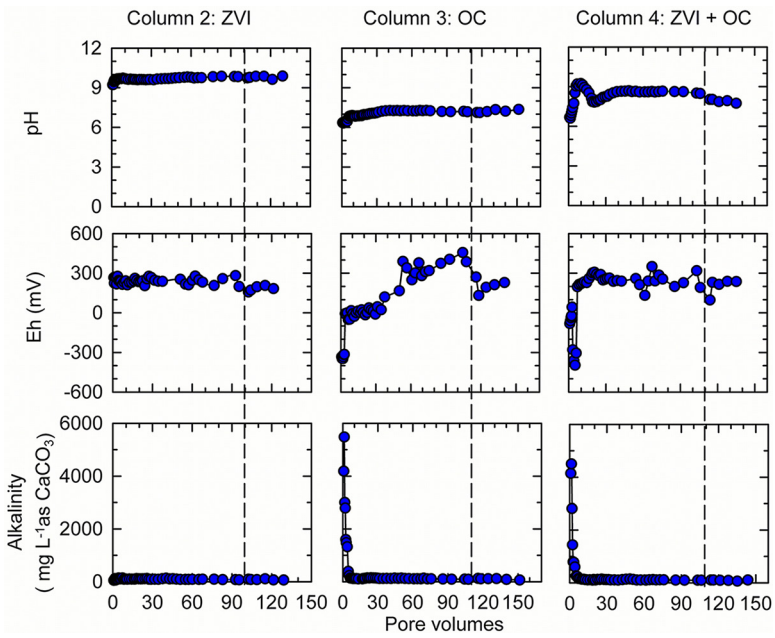

Fig. 3. Values of pH, Eh, and concentrations of alkalinity as a function of pore volumes (PV) in effluent from columns containing zero-valent Fe (ZVI), organic C (OC), or both; the dashed lines indicate a change in flow rate in each column, dividing the experiment into two stages.

(Fig. 1). Similarly, in the second stage of the experiment when the flow rate was lowered, OC combined with ZVI exhibited more uniform removal of ClO_4^- in Column 4 than Column 3. The concentration of ClO_4^- in the effluent of Column 4 decreased from 679 μg L^{-1} after 106 PV in the first stage of the experiment to 1.37 μg L^{-1} after 144 PV in the second stage of the experiment. Previous studies have suggested the pathway for biological degradation of ClO_4^- (Rikken et al., 1996) as shown in Fig. 5.

The first two reactions are catalyzed by (per) chlorate reductase. Chlorite dismutase catalyzes the disproportionation of ClO_2^- into Cl^- and O_2 (Okeke and Frankenberger, 2003). The OC probably provided sufficient C and N for microbial degradation of ClO_4^- in Columns 3 (OC) and 4 (ZVI + OC); however, complete removal of ClO_4^- was not consistently observed until the second stage of the experiment (Fig. 1). Extensive removal of ClO_4^- initially was observed in Column 3, but the rate of ClO_4^- removal declined after 30 PVs. After the flow rate decreased, complete removal of ClO_4^- was observed. Initially, little ClO_4^- removal was observed in Column 4. More extensive removal was observed after 10 PVs, suggesting that a period of acclimation was required before ClO_4^- reduction was established. After 60 PVs, the rate of ClO_4^- removal declined, suggesting depletion of labile OC. During Stage 2 of the experiment, complete removal of ClO_4^- was observed, suggesting that the rate of OC fermentation was sufficient to provide labile OC for sustained ClO_4^- reduction.

Chloride, the final potential product of ClO_4^- biological degradation, should be released at an amount equivalent to the mass of ClO_4^- removed. In contrast to Column 2 (ZVI), the concentrations of Cl in the first 2 PV effluents of Columns 3 (OC) and 4 (ZVI + OC) were below the detection limit (0.01 mg L^{-1}), probably due to the flushing and saturation of the columns before the experiment and the small fraction (10% v/v) of ZVI in Column 4 (ZVI + OC) compared with that of ZVI (50% v/v) in Column 2 (ZVI). The changes in Cl^- concentrations in both Columns 3 (OC) and 4 (ZVI + OC) effluent were inversely correlated to ClO_4^- concentrations. Very consistent concentrations of total effluent Cl (sum of ClO_4^- and Cl, in μmol L^{-1}) relative to the input ClO_4^- concentrations for these columns indicated that the expected mass of Cl was accounted for in both Columns 3 and 4 (Fig. 4).

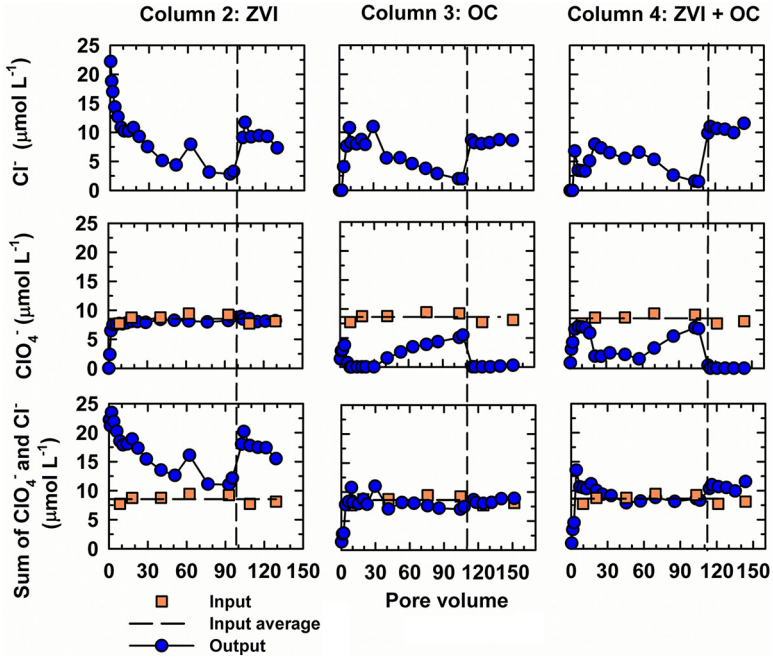

Fig. 4. Concentrations of Cl^-, ClO_4^-, and total Cl (sum of Cl^- and ClO_4^-) as a function of pore volumes in effluent from columns containing zero-valent Fe (ZVI), organic C (OC), or both; the dashed lines indicate a change in flow rate in each column, dividing the experiment into two stages.

Removal Rates of Nitrate and Perchlorate within Columns

The two NO_3^- and ClO_4^- profiles collected for each of Columns 2, 3, and 4 in the second stage of the experiment were similar (Fig. 6). Therefore, only the profiles measured in the first stage of the experiment (95.4 PV for Column 2, 108 PV for Column 3, and 106 PV for Column 4) and one of the profiles measured in the second stage of the experiment (115 PV for Column 2, 132 PV for Column 3, and 128 PV for Column 4) were used for calculation of the removal rate parameters.

Nitrate removal rates within Columns 2, 3, and 4 were consistent with a first-order rate model (Fig. 7), as reported in other studies (Appelo and Postma, 2005; Tan et al., 2004):

$$C = C_0 \exp(-k_1 t) \quad [5]$$

$$R_N = k_1 C \quad [6]$$

where C is the NO_3^- concentration (mg L^{-1}), C_0 is the initial NO_3^- concentration (mg L^{-1} or mmol L^{-1}), k_1 is a first-order rate constant (d^{-1}), t is the residence time (d), and R_N is the reaction rate (removal rate) of NO_3^- (mg L^{-1} d^{-1} or mmol L^{-1} d^{-1}). The best-fit NO_3^- degradation equation based on calculated residuals for each column (SigmaPlot, SPSS Inc.) was selected from the two first-order expressions derived from the two stages of the experiment.

Nitrate removal by ZVI within Column 2 (ZVI) followed a first-order removal model, with removal rates of $R_{N,2} = 0.015C$ mmol L^{-1} d^{-1} in the first stage of the experiment and $R_{N,2} = 0.011C$ mmol L^{-1} d^{-1} in the second stage of the experiment (Table 2; Fig. 7); however, neither of these equations could adequately describe the degradation curves in both experimental stages. An average first-order removal rate of $R_{N,2} = 0.013C$ mmol L^{-1} d^{-1}, which fell between the first- and second-stage data sets, is recommended to best describe the NO_3^- removal within Column 2 (ZVI).

The denitrification rate within Column 3 (OC) can be described by $R_{N,3} = 0.010C$ mmol L^{-1} d^{-1} (Table 2; Fig. 7). Both

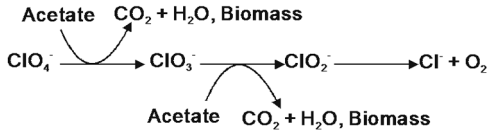

Fig. 5. Suggested pathway for biological degradation of ClO_4^- (Rikken et al., 1996).

zero-order and first-order rate expressions have been observed to provide reasonable descriptions of the rate of denitrification (R^2 > 0.86) (Tan et al., 2004). Similar findings were observed in this study: NO_3^- removal by ZVI and OC in Column 4 in both the first and second stages of the experiment were consistent with both the first-order and zero-order rate equations in terms of R^2 (>0.94) (Table 2; Fig. 7). However, to maintain consistency between the NO_3^- removal rates for Column 4 (ZVI + OC) and those for Column 2 (ZVI) and Column 3 (OC), $R_{N,4} = 0.025C$ mmol L^{-1} d^{-1} was used to describe the rates of NO_3^- removal in Column 4 throughout the experiment. Given the same initial concentration, NO_3^- was removed much more rapidly in Column 4 than in Columns 2 or 3 (Fig. 6).

Perchlorate removal in some bioreactors has been observed to follow first-order reaction rates with respect to ClO_4^- concentration (Min et al., 2004). In this study, however, ClO_4^- removal in Columns 3 (OC) and 4 (ZVI + OC) followed zero-order rate equations (Fig. 8):

$$C = -k_0 t \quad [7]$$

where C is the ClO_4^- concentration (μg L^{-1} or μmol L^{-1}), t is the residence time (d), and k_0 is a zero-order rate constant for ClO_4^- removal (μg L^{-1} d^{-1} or μmol L^{-1} d^{-1}). The best-fit equation for ClO_4^- removal, based on least squares regression, was also obtained using a zero-order rate expression derived from the two stages of the experiment. The ClO_4^- removal rate within Column 3 (OC) was $R_{P,3}$ = 0.61 μmol L^{-1} d^{-1} for 0 < x < 2.9 d (derived from the distance between the column input and the sampling point) and NO_3^- concentration >2 mg L^{-1} (NO_3–N). The ClO_4^- removal rates were $R_{P,3}$ = 1.95 μmol L^{-1} d^{-1} in the first stage of the experiment and $R_{P,3}$ = 1.84 μmol L^{-1} d^{-1} in the second stage of the experiment, where 2.9 < t < 6.7 d (for a NO_3^- concentration <2 mg L^{-1} NO_3–N). Neither of these removal rates adequately described the observations from both experimental stages. An average zeroth-order removal rate of $R_{P,3}$ = 1.89 μmol L^{-1} d^{-1} was selected to describe the ClO_4^- removal rate within Column 3 (OC) for 2.9 < t < 6.7 d and NO_3^- <2 mg L^{-1} NO_3–N. The overall ClO_4^- removal rate within Column 4 (ZVI + OC) was $R_{P,4}$ = 1.14 μmol L^{-1} d^{-1} (Table 2; Fig. 6 and 8). The ClO_4^- removal rate for the second stage of the Column 4 experiment was $R_{P,4}$ = 0.94 μmol L^{-1} d^{-1} for 0 < t < 2.0 d and NO_3^- concentration >2 mg L^{-1} NO_3–N. A statistical comparison of the ClO_4^- removal rates for Columns 3 (OC) and 4 (ZVI + OC) indicated that ClO_4^- was removed more rapidly in Column 4 (ZVI + OC) than in Column 3 (OC) for NO_3^- > 2 mg L^{-1} (NO_3–N) in the second stage of the experiment (Fig. 6 and 8) but more rapidly in Column 3 for NO_3^- <2 mg L^{-1} NO_3–N.

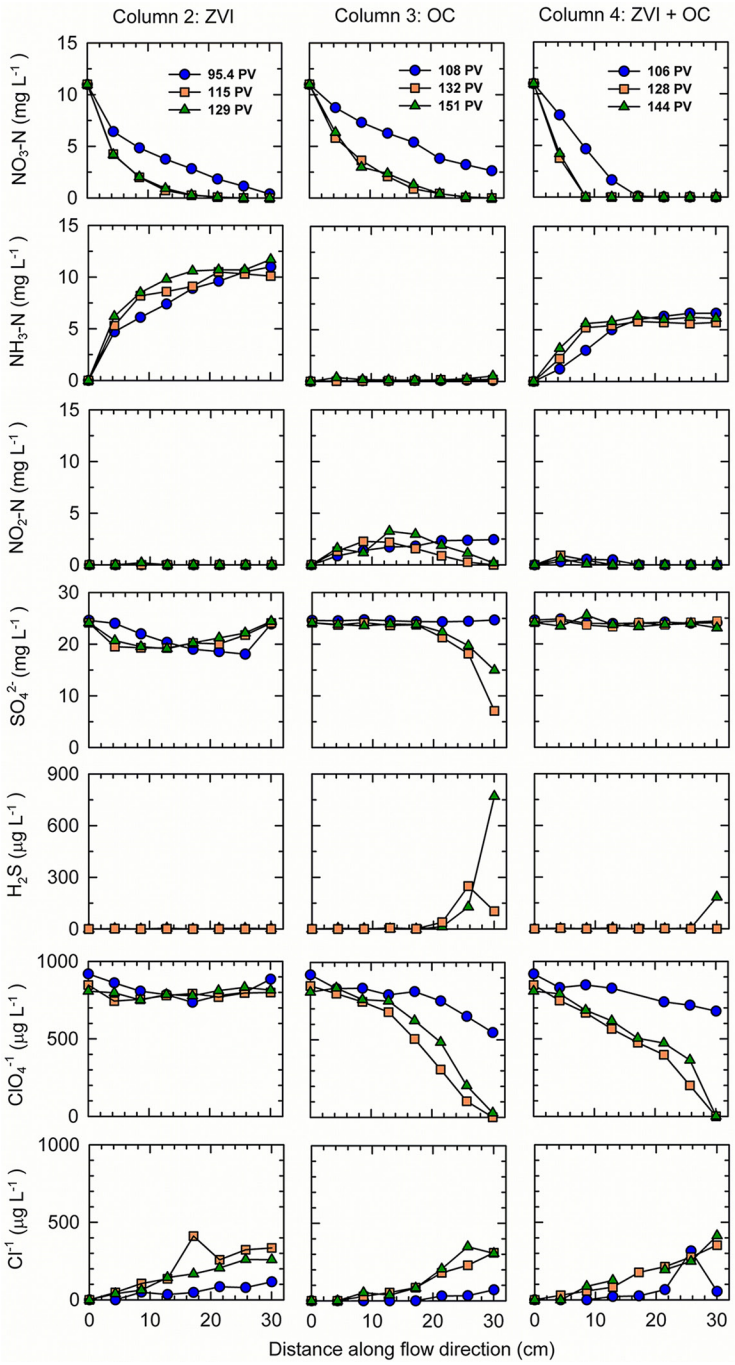

Fig. 6. Concentrations of NO_3–N, NH_3–N, NO_2–N, SO_4^{2-}, H_2S, ClO_4^-, and Cl^- as a function of distance along flow direction within columns containing zero-valent Fe (ZVI), organic C (OC), or both. Blue circle symbols represent data collected during the first stage of the experiment, while orange square and green triangle symbols represent data collected during the second stage of the experiments, given in terms of pore volumes (PV).

Effect of Nitrate and Sulfate on Perchlorate Removal Rate

The impact of NO_3^- on ClO_4^- reduction is important because NO_3^- is a common co-contaminant in ClO_4^-–contaminated water (Xu et al., 2003). Most ClO_4^-–reducing bacteria are also denitrifiers, and the simultaneous removal of NO_3^- and ClO_4^- from contaminated waters has been observed (Logan and LaPoint, 2002; Min et al., 2004). Likewise, the NO_3^- and ClO_4^- within Columns 3 (OC) and 4 (ZVI + OC) were removed simultaneously. However, the overall NO_3^- removal within both Columns 3 and 4 occurred at a more rapid rate than ClO_4^- removal (Fig. 6), which may have been due to competition for common electron donors (organic matter) between the two removal processes (Chung et al., 2010). The selection of electron acceptors by microorganisms is competitive to maximize the energy yield in a redox reaction. Nitrate reduction was found to

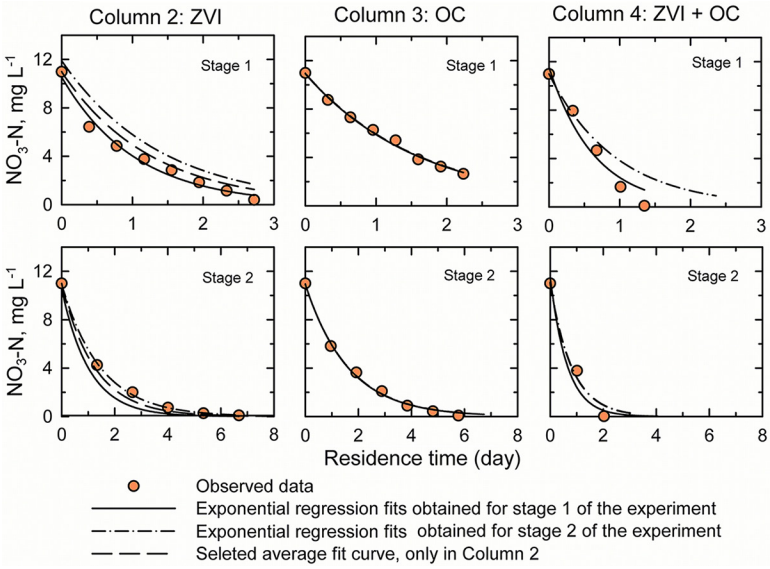

Fig. 7. Regression fits of NO_3–N removal as a function of residence time in columns containing zero-valent Fe (ZVI), organic C (OC), or both.

be more thermodynamically favored over ClO_4^- reduction due to the lower electron transfer requirement for NO_3^- reduction compared with that for ClO_4^- reduction (Chung et al., 2010). The ClO_4^-–reducing bacteria preference of O_2 or NO_3^- over ClO_4^- has been reported (Roldan et al., 1994). Moreover, if the same enzyme in a microorganism was used for both NO_3^- and ClO_4^- reductions, NO_3^- was likely to inhibit ClO_4^- reduction and ClO_4^- was also likely to inhibit NO_3^- reduction, depending on the initial concentrations of NO_3^- and ClO_4^- (Giblin and Frankenberger, 2001). Complete NO_3^- removal within Columns 3 and 4 was observed before complete ClO_4^- removal (Fig. 6), which is similar to other studies (Min et al., 2004).

Nitrate has different effects on ClO_4^- removal rates. Nitrate was found to inhibit the ClO_4^- reduction rate in some studies (Brown et al., 2002; Xu et al., 2003) but not others (Giblin et al., 2000). In this study, the inhibition of ClO_4^- removal by NO_3^- was observed within Column 3 (OC) but not Column 4 (ZVI + OC). The inhibiting effects of NO_3^- on ClO_4^- removal occurred at NO_3^- concentrations >2 mg L^{-1} NO_3–N within Column 3 (OC) during the second stage of the experiment when flow rate was maintained at 0.1 PV d^{-1}. Moreover, rapid ClO_4^- degradation did not proceed until NO_3^- concentrations were reduced to relatively low levels (normally <2 mg L^{-1} NO_3–N), which is consistent with previous findings (Tan et al., 2004). However, the presence of NO_3^- within Column 4 (ZVI + OC) did not inhibit ClO_4^- removal (Fig. 6), which followed similar linear rates in the presence and absence of NO_3^-. These results suggest that adding ZVI to wood chips can potentially reduce the inhibition of NO_3^- (>2 mg L^{-1} NO_3–N) on ClO_4^- removal when the flow rate was maintained at 0.1 PV d^{-1}. The presence of SO_4^{2-} did not inhibit ClO_4^- removal in Column 3 (OC) or 4 (ZVI + OC) (Fig. 6), as is consistent with previous reports (Chung et al., 2010).

Conclusions

Reactive media containing OC or a mixture of ZVI + OC were found effective for removing NO_3^- and ClO_4^- from water. The removal of NO_3^- and ClO_4^- followed first-order and zero-order rates in these column experiments, respectively. Nitrate and

Table 2. Nitrate and ClO_4^- removal rates calculated using least-squares regression during two experimental stages.

Contaminant	Column	Stage†	Removal rate‡	Recommended fit§	Half-life	R^2
			mmol L^{-1} d^{-1}		d	
NO_3–N	2	1	0.015 × *C*		0.7	0.983
		2	0.011 × *C*		1.0	0.999
		avg.	0.013 × *C*	§	0.8	–¶
	3	1	0.010 × *C*	§	1.1	0.993
		2	0.010 × *C*		1.1	0.997
	4	1	0.025 × *C*	§	0.4	0.947
		2	0.017 × *C*		0.7	0.985
			μmol L^{-1} d^{-1}			
ClO_4^-	3	1	1.41		3.1	0.890
		2	1.36	§	3.2	0.950
		1	1.21 (0–12.9 cm)		3.6	0.833
		2	0.61 (0–12.9 cm)	§	7.0	0.999
		1	1.95 (12.9–30 cm)		2.2	0.882
		2	1.84 (12.9–30 cm)		2.3	0.991
		avg.	1.89 (12.9–30 cm)	§	2.3	–
	4	1	0.93		4.6	0.945
		2	1.14	§	3.8	0.968

† Removal rates were calculated for either Stage 1 or 2 of the experiment or the average of the two stages, where indicated.

‡ *C* is the input NO_3–N concentration; the reported rates were calculated for the entire length of the columns, except where the column distance range is provided. The distance 0–12.9 cm corresponds to NO_3–N concentrations >2 mg L^{-1} and the distance 12.9–30 cm corresponds to NO_3–N concentrations <2 mg L^{-1}.

§ Recommended rates that provide the best fits for both stages of the experiments.

¶ Not applicable.

ClO_4^- were removed simultaneously within the columns; however, complete NO_3^- removal occurred before complete ClO_4^- removal. Addition of ZVI to wood chips reduced the inhibition of NO_3^- (>2 mg L^{-1} NO_3–N) on ClO_4^- degradation when the flow rate was maintained at 0.1 PV d^{-1}. Decreasing the flow rate from 0.5 to 0.1 PV d^{-1} resulted in more complete removal of NO_3^-, SO_4^{2-}, and ClO_4^-. These results suggest that permeable reactive barriers and bioreactors containing OC or mixtures of OC and ZVI may be suitable for treating NO_3^-, ClO_4^-, and SO_4^{2-} at mining and blasting sites.

Acknowledgments

Funding for this research was provided by the Ontario Ministry of Research and Innovation—Ontario Research Excellence Fund and the Natural Sciences and Engineering Research Council of Canada. Laura Groza and Joy Hu provided assistance with the perchlorate and anion analyses. Additional technical support was provided by Peng Liu.

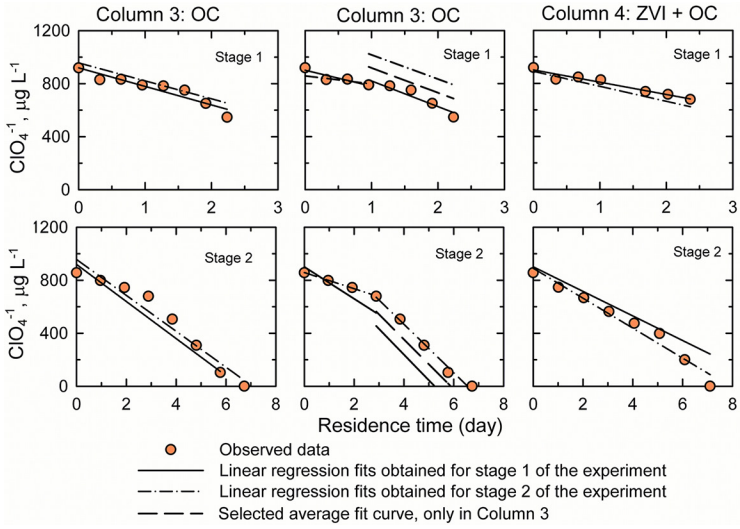

Fig. 8. Regression fits of ClO_4^- removal as a function of residence time in columns containing organic C (OC) and both zero-valent Fe (ZVI) and OC.

References

APHA. 2005. Method 4500: NH_3 nitrogen (ammonia). APHA, Washington, DC.

Appelo, C.A.J., and D. Postma. 2005. Geochemistry, groundwater and pollution. AA Balkema, Rotterdam, the Netherlands.

Bailey, B.L., L.J.D. Smith, D.W. Blowes, C.J. Ptacek, L. Smith, and D.C. Sego. 2013. The Diavik Waste Rock Project: Persistence of contaminants from blasting agents in waste rock effluent. Appl. Geochem. 36:256–270. doi:10.1016/j.apgeochem.2012.04.008

Blowes, D.W., C.J. Ptacek, S.G. Benner, C.W.T. McRae, T.A. Bennett, and R.W. Puls. 2000. Treatment of inorganic contaminants using permeable reactive barriers. J. Contam. Hydrol. 45:123–137. doi:10.1016/S0169-7722(00)00122-4

Borden, R.C. 2007. Concurrent bioremediation of perchlorate and 1,1,1-trichloroethane in an emulsified oil barrier. J. Contam. Hydrol. 94:13–33. doi:10.1016/j.jconhyd.2007.06.002

Brown, J.C., V.L. Snoeyink, and M.J. Kirisits. 2002. Abiotic and biotic perchlorate removal in an activated carbon filter. J. Am. Water Works Assoc. 94:70–79.

Chung, J., S. Shin, and J. Oh. 2010. Influence of nitrate, sulfate and operational parameters on the bioreduction of perchlorate using an up-flow packed bed reactor at high salinity. Environ. Technol. 31:693–704. doi:10.1080/09593331003621557

Evans, P.J., and M.M. Trute. 2006. In situ bioremediation of nitrate and perchlorate in vadose zone soil for groundwater protection using gaseous electron donor injection technology. Water Environ. Res. 78:2436–2446. doi:10.2175/106143006X123076

Gal, H., Z. Ronen, N. Weisbrod, O. Dahan, and R. Nativ. 2008. Perchlorate biodegradation in contaminated soils and the deep unsaturated zone. Soil Biol. Biochem. 40:1751–1757. doi:10.1016/j.soilbio.2008.02.015

Giblin, T., and W.T. Frankenberger, Jr. 2001. Perchlorate and nitrate reductase activity in the perchlorate-respiring bacterium perclace. Microbiol. Res. 156:311–315. doi:10.1078/0944-5013-00111

Giblin, T.L., D.C. Herman, M.A. Deshusses, and W.T. Frankenberger, Jr. 2000. Removal of perchlorate in ground water with a flow-through bioreactor. J. Environ. Qual. 29:578–583. doi:10.2134/jeq2000.00472425002900020028x

Hunter, W.J. 2002. Bioremediation of chlorate or perchlorate contaminated water using permeable barriers containing vegetable oil. Curr. Microbiol. 45:287–292. doi:10.1007/s00284-002-3751-4

Leung, A.M., E.N. Pearce, and L.E. Braverman. 2010. Perchlorate, iodine and the thyroid. Best. Pract. Res., Clin. Endocrinol. Metab. 24:133–141. doi:10.1016/j.beem.2009.08.009

Light, T. 1972. Standard solution for redox potential measurements. Anal. Chem. 44:1038–1039. doi:10.1021/ac60314a021

Lindsay, S.S., and M.J. Baedecker. 1988. Determination of aqueous sulfide in contaminated and natural water using the methylene blue method. In: A.G. Collins and A.I. Johnson, editors, Ground-water contamination: Field methods. ASTM, West Conshohocken, PA. p. 349–357.

Lindsay, M.B.J., K.D. Wakeman, O.F. Rowe, B.M. Grail, C.J. Ptacek, D.W. Blowes, and D.B. Johnson. 2011. Microbiology and geochemistry of mine tailings amended with organic carbon for passive treatment of pore water. Geomicrobiol. J. 28:229–241. doi:10.1080/01490451.2010.493570

Logan, B.E., and D. LaPoint. 2002. Treatment of perchlorate- and nitrate-contaminated groundwater in an autotrophic, gas phase, packed-bed bioreactor. Water Res. 36:3647–3653. doi:10.1016/S0043-1354(02)00049-0

Min, B., P.J. Evans, A.K. Chu, and B.E. Logan. 2004. Perchlorate removal in sand and plastic media bioreactors. Water Res. 38:47–60. doi:10.1016/j.watres.2003.09.019

Nordstrom, D.K. 1977. Thermochemical redox equilibria of ZoBell's solution. Geochim. Cosmochim. Acta 41:1835–1841. doi:10.1016/0016-7037(77)90215-0

Okeke, B.C., and W.T. Frankenberger, Jr. 2003. Molecular analysis of a perchlorate reductase from a perchlorate-respiring bacterium perclace. Microbiol. Res. 158:337–344. doi:10.1078/0944-5013-00213

Okeke, B.C., and W.T. Frankenberger, Jr. 2005. Use of starch and potato peel waste for perchlorate bioreduction in water. Sci. Total Environ. 347:35–45. doi:10.1016/j.scitotenv.2004.12.041

Okeke, B.C., T.L. Giblin, and W.T. Frankenberger, Jr. 2002. Reduction of perchlorate and nitrate by salt tolerant bacteria. Environ. Pollut. 118:357–363. doi:10.1016/S0269-7491(01)00288-3

Rahman, A., and A. Agrawal. 1997. Reduction of nitrate and nitrite by iron metal: Implications for ground water remediation. In: Book of abstracts: 213th American Chemical Society National Meeting, San Francisco, CA. 13–17 Apr. 1997. ACS, Washington, DC. p. 13–17.

Rikken, G.B., A.G.M. Kroon, and C.G. van Ginkel. 1996. Transformation of (per) chlorate into chloride by a newly isolated bacterium: Reduction and dismutation. Appl. Microbiol. Biotechnol. 45:420–426. doi:10.1007/s002530050707

Robertson, W.D., C.J. Ptacek, and S.J. Brown. 2007. Geochemical and hydrogeological impacts of a wood particle barrier treating nitrate and perchlorate in ground water. Ground Water Monit. Rem. 27:85–95. doi:10.1111/j.1745-6592.2007.00140.x

Roldan, M.D., F. Reyes, C. Moreno-Vivian, and F. Castillo. 1994. Chlorate and nitrate reduction in the phototrophic bacteria *Rhodobacter capsulatus* and *Rhodobacter sphaeroides*. Curr. Microbiol. 29:241–245. doi:10.1007/BF01570161

Snyder, S.A., B.J. Vanderford, and D.J. Rexing. 2005. Trace analysis of bromate, chlorate, iodate, and perchlorate in natural and bottled waters. Environ. Sci. Technol. 39:4586–4593. doi:10.1021/es047935q

Srinivasan, R., and G.A. Sorial. 2009. Treatment of perchlorate in drinking water: A critical review. Sep. Purif. Technol. 69:7–21. doi:10.1016/j.seppur.2009.06.025

Tan, K., T.A. Anderson, and W.A. Jackson. 2004. Degradation kinetics of perchlorate in sediments and soils. Water Air Soil Pollut. 151:245–259. doi:10.1023/B:WATE.0000009904.23410.89

Till, B.A., L.J. Weathers, and P.J.J. Alvarez. 1998. Fe(0)-supported autotrophic denitrification. Environ. Sci. Technol. 32:634–639. doi:10.1021/es9707769

Toride, N., F.J. Leij, and M.Th. van Genuchten. 1995. The CXTFIT code for estimating transport parameters from laboratory or field tracer experiments. U.S. Salinity Lab., Riverside, CA.

Wang, Y., L. Jin, M.A. Deshusses, and M.R. Matsumoto. 2013. The effects of various amendments on the biostimulation of perchlorate reduction in laboratory microcosm and flowthrough soil columns. Chem. Eng. J. 232:388–396. doi:10.1016/j.cej.2013.07.060

Ward, C.H. 2008. In situ bioremediation of perchlorate in groundwater. Springer, New York.

Xu, J., Y. Song, B. Min, L. Steinberg, and B.E. Logan. 2003. Microbial degradation of perchlorate: Principles and applications. Environ. Eng. Sci. 20:405–422. doi:10.1089/109287503768335904

Yu, X., C. Amrhein, M.A. Deshusses, and M.R. Matsumoto. 2006. Perchlorate reduction by autotrophic bacteria in the presence of zero-valent iron. Environ. Sci. Technol. 40:1328–1334. doi:10.1021/es051682z